Detecting Lesion Characteristics of Diabetic Retinopathy Using Machine Learning and Computer Vision

Alhadi Bustamam, Devvi Sarwinda, Bariqi Abdillah, Tesdiq P. Kaloka
Universitas Indonesia
Depok, West Java, 16424
Indonesia
{alhadi@sci.ui.ac.id} {devvi@sci.ui.ac.id} {tesdiq@sci.ui.ac.id} {bariqi.abdillah@sci.ui.ac.id}

ABSTRACT: *One indicator of the severity of diabetic retinopathy is the existence of lesion characteristics in the eyes such as microaneurysm, haemorrhages, exudates, and neovascularization. Without proper early medical attention, this lesion could lead to blindness. Considering its importance, a system that could detect such lesion will be beneficial. This paper investigates lesion characteristics of diabetic retinopathy from fundus images such as microaneurysm (redsmalldots), exudates, haemorhages, and neovascularization. In this study, we present three of feature extraction methods, i.e., Local Binary Pattern (LBP), Gray Level Co-Occurrence Matrix (GLCM) and Segmentation Fractal Texture Analysis (SFTA). K-Nearest Neighbor (KNN) and Support Vector Machine (SVM) chosen as classifiers for classifying five classes (redsmalldots, haemorrhages, hard exudates, soft exudates, and neovascularization). The data used in this research obtained from DiaretDB0 database. The experimental results show that our proposed method can detect the lesion characteristics of diabetic retinopathy with a higher accuracy of 86,84% and 96% for SVM and KNN respectively.*

Keywords: Diabetic Retinopathy, LBP, GLCM, SFTA, KNN, SVM

Received: 8 September 2019, Revised 29 November 2019, Accepted 5 December 2019

DOI: 10.6025/jes/2020/10/1/23-33

1. Introduction

In the last 20 years, the number of people diagnosed with diabetes has risen by approximately 300%. Diabetes can occur when insulin, the hormone that regulates blood sugar, is neither being correctly produced nor being used effectively by the pancreas. Diabetes can make some complication in the nerve and blood vessels. Diabetic retinopathy is one of the diabetes complications [1], where one of three people with diabetes, would likely have diabetic retinopathy and get vision problem from this disease [2].

There are two stages of diabetic retinopathy. The first stage or early step is Non-Proliferative Diabetic Retinopathy (NPDR). NPDR consist of mild, moderate, and severe conditions. The next stage of diabetic retinopathy is Proliferative Diabetic Retinopathy (PDR), which is leading to blindness. By evaluating the lesion on the retina, it could be used as a parameter to recognize diabetic retinopathy. Some indications of NPDR stage are:

• There are some spots in the form of venous dilatation

• Microaneurysms

• Hard and soft exudates

• Bleeding in intraretinal microvascular

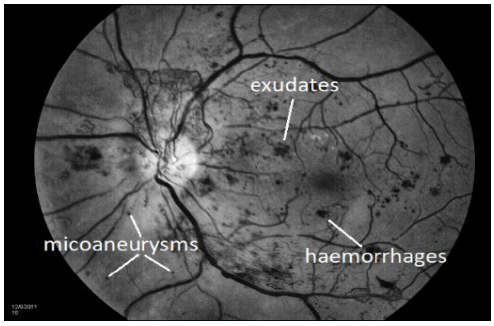

Figure 1. Lesion characteristics in the fundus image

The PDR is an advanced stage of NPDR phase, which is characterized by the appearance of the neovascular blood vessel. Leakage from tiny blood vessels of the retina can cause microaneurysms and has a red circular shape. Haemorrhages appeared after microaneurysms get ruptured.

Some of the lesion that has lipids and proteins can become hard and soft exudates. The color of hard exudates is predominantly white, while soft exudates are mostly yellow color [3]. The characteristics of lesion in fundus image can be seen in Figure 1.

Many works have been done regarding diabetic retinopathy classification using lesion. SVM and Bayesian Classifier are used by [4] to make classification of diabetic retinopathy with an accuracy of 95% and 90% respectively. Another work by [5], proposing a new limit for detecting lesion location with 96.7% sensitivity and specificity of 94.2%. Meanwhile, another method by [6] propose exudate features indicating disease progression towards dangerous convergence method for early detection of diabetic retinopathy with an accuracy of 92%. Previous work from [7] classifies diabetic retinopathy using four phase classifications, LBP, GLCM, GM-LBP, and NM-LBP. Another classification approach based on successive clutter-rejection by [8] manage to achieve 90% sensitivity.

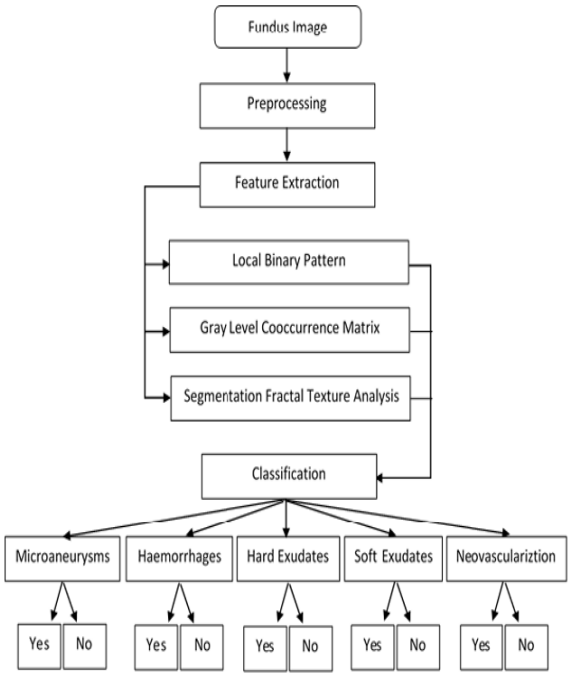

Figure 2. Flowchart for the proposed method

In this study, we aim to detect each lesion characteristics based on its images such as microaneurysm (redsmalldots), exudates, haemorrhages, and neovascularization. We employ several texture features and various classification method to compare each effectiveness. Furthermore, we use Local Binary Pattern (LBP), Gray Level Co-occurrence Matrix (GLCM) and Segmentation Fractal Texture Analysis for our feature extraction method (SFTA). Finally, we implement K-Nearest Neighbors (KNN) and Support Vector Machines (SVM) as our classifier.

The explanation of the material and methods used in this study is in Section II, such as the preprocessing method (CLAHE), features extraction methods (LBP, SFTA, and GLCM) and classification method (KNN and SVM). In Section III, we describe the results of each combination of feature extraction methods and classification methods, while in Section IV we conclude our experimental results.

2. The Material and Method

There has been some research that addresses the problem of classification of normal and abnormality in diabetic retinopathy. Normally, the classification based on lesion characteristic of diabetic retinopathy using texture features extracted from the image. In this study, several feature extractions such as Local Binary Pattern (LBP), Gray Level Co-Occurrence Matrix (GLCM), and Segmentation Fractal Texture Analysis (SFTA) specifically are used.

Firstly, the obtained images were converted into grayscale. Then, in order to improve the quality of the image, we employ Contrast Limited Adaptive Histogram Equalization (CLAHE). After the preprocessing step is done, we extract the feature from each image. This feature will be used as training and testing dataset for our model. We train our model using K-Nearest Neighbors (K-NN) and Support Vector Machine (SVM). The overall process can be seen in Figure 2. Now we discuss the methods in the working model, following CLAHE, LBP, GLCM, KNN, and SVM.

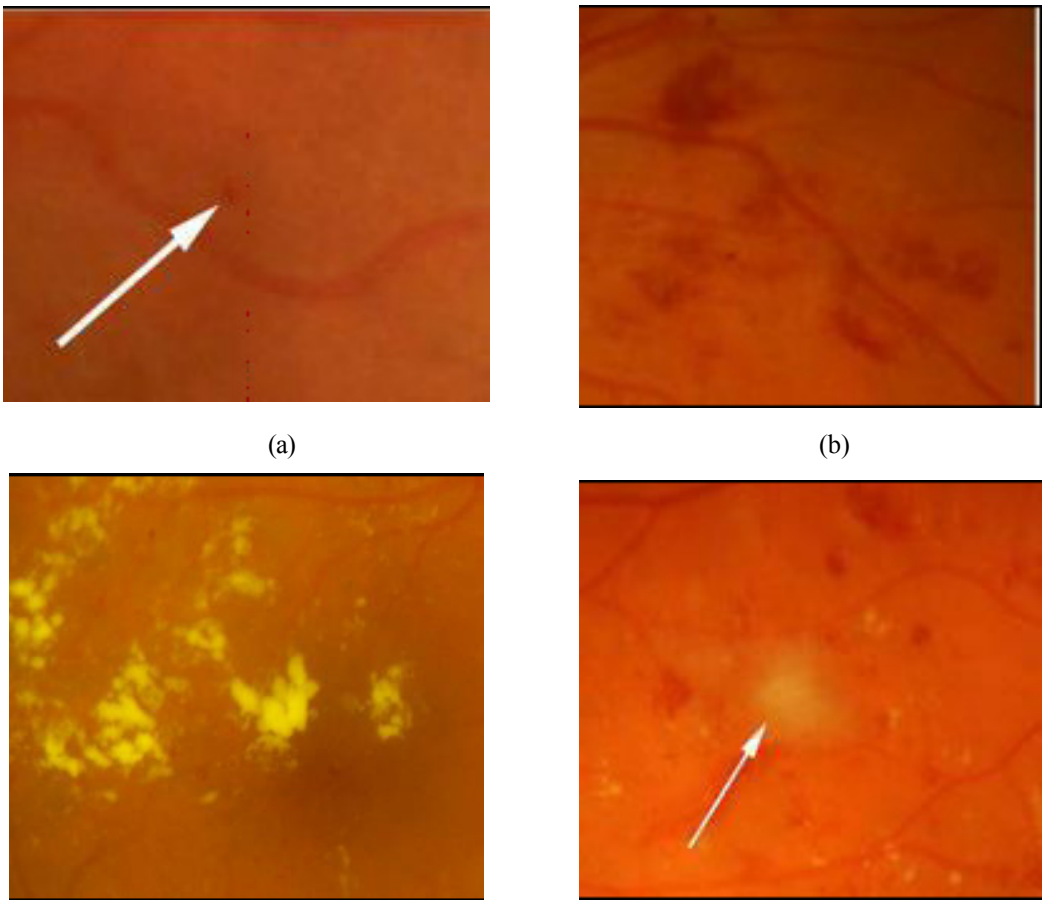

(a) (b)

(c) (d)

(e)

Figure 3. The lesion characteristics of diabetic retinopathy. (a) red small dots; (b) haemorrhages; (c) hard exudates; (d) soft exudates; (e) neovascularization [9]

2.1. Data Acquisition

We used data from DiaretDB0 database, contains 130 fundus images, in which 106 has microaneurysms and 24 not, 80 has haemorrhages and 50 not, 71 with hard exudates and B. *Contrast Limited Adaptive Histogram Equalization (CLAHE)* 59 not, 41 with soft exudates and 89 not, 20 has neovascularization, and 110 is not [9]. In this study, the five lesion characteristics of diabetic retinopathy can be seen in Figure 3.

The problem of delay in diagnosis or medication errors associated with diabetic retinopathy caused by limited contrast of lesion image in diabetic retinopathy [10]. In these cases, histogram equalization can play as an important role.

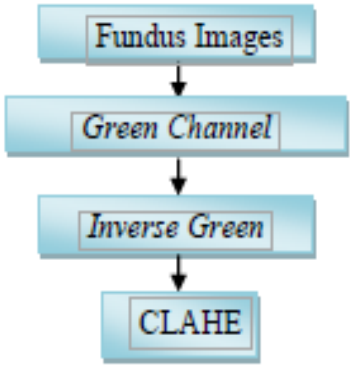

Figure 4. Scheme of our preprocessing method

Histogram modification is used to obtain the desired image histogram. One technique that could be used for histogram enhancement is CLAHE. Histogram equalization changes the intensity of the image to the uniform. Histogram equalization made by changing the gray degree of a pixel *(r)* and a new gray degree *(s)* with a *T* transformation function. CLAHE performs adaptive calculations per pixel to determine its new gray value.

$$S = T(r) \tag{1}$$

In this step, before we implement the CLAHE method for our preprocessing method, we extract the image to green channel frame. Green channel is known has good contrast than another frame in color images. The scheme of our preprocessing method could see in Figure 4.

In this study, we did preprocess for each image to see lesion characteristics. In Figure 5 and 6, the result of image preprocessing

for microaneurysm and exudates. From Figure 5 and 6, we can see the difference of microaneurysm (redsmalldots) and exudates.

2.2. Local Binary Pattern (LBP)

Local Binary Pattern (LBP) is straightforward feature extraction, yet very effective. Which labels each pixel in an image by thresholding the neighborhood of each pixel and coded the result as a binary representation. The value will assign into 0 if the center of the pixel is greater than its neighborhood and 1 otherwise [11]. For each pixel, it should be code into a 9d binary array, with 256 different possible labels for each pixel. The value of the LBP code of a pixel $(x_c, y_c)$was given by:

$$LBP_{P,R} = \sum_{P=0}^{P-1} sign\,(g_p - g_c)2^p \tag{2}$$

and

$$sign\,(x) = \begin{cases} 1, & x \geq 0 \\ 0, & x < 0 \end{cases} \tag{3}$$

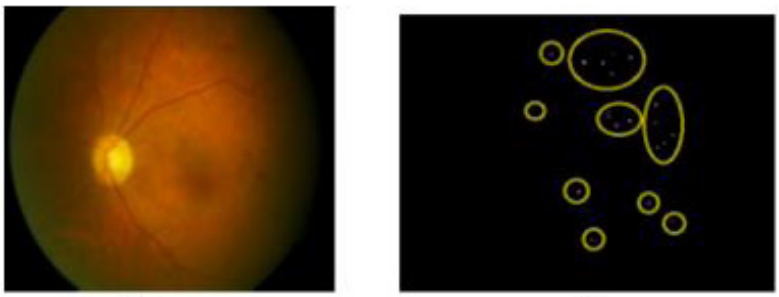

Figure 5. Image Preprocessing for microaneurysm. (a) original sample images from DiaretDB0; (b) result of preprocessing

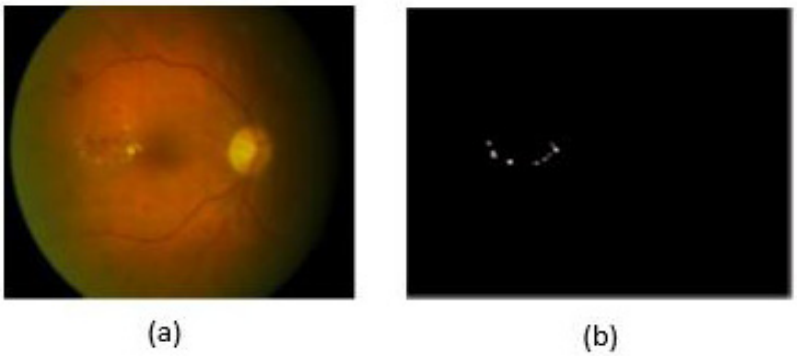

Figure 6. Image Preprocessing for exudates. (a) original sample images from Diaret DB0; (b) result of preprocessing

With the number of neighbors is P and the radius is R [12]. Illustration for basic LBP could see in Figure 7. The pixel set to 0, if g_p is smaller than g_c otherwise set to 1. To get 8-bit value, all the results are combined.

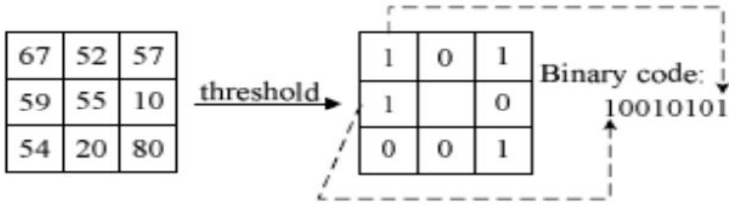

Figure 7. Basic LBP operator Illustration

Figure 8 illustrate Equation (2), how to calculate the pixel's circular neighborhoods from the LBP operator *(r=1, p=8)*. We reduced the number of possibility pattern using concept of uniform pattern in LBP. LBP is called uniform if the binary pattern consists of maximum two bitwise transitions from 0 to 1 or otherwise. For example, 11111111 is uniform because it has no transition, 11000000 is uniform because it has one transition from 1 to 0, meanwhile 01010100 is not uniform because it has six transitions [13]. By using uniform pattern concept, we can reduce 198 patterns out of 256 patterns into 58 patterns [14].

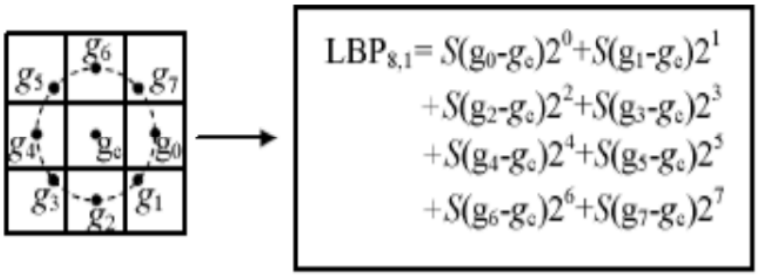

Figure 8. Pixel's circular neighborhoods from the LBP operator (*r=1*, *p=8*)

2.3. Gray Level Co-Occurrence Matrix (GLCM)

GLCM is a statistical method that used to extract texture feature. GLCM value obtained from the value of the co-occurrence matrix with the joint probability density of two pixels which have different positions [15]. The pixel value of grayscale is calculated based on the summation of the relation contrast. In GLCM, local pattern of an image analyzed. GLCM was also known as a texture descriptor. Many researchers used GLCM to process medical image.

GLCM expresses the spatial relationship or distribution between two pixels adjacent to the intensity of each *i* and *j*, distance, and angle. GLCM denoted by $P_d(i, j)$ Adjacent pixels have a distance *d* and eight different directions (00, 450, 900, 1350, 1800, 2250, 2700, 3150). Figure 9 shows the direction of neighboring pixels.

In this work, we use Contrast, Correlation, Energy, and Homogeneity for the features from GLCM. The Equation of the features described in Equation (4), (5), (6), and (7).

$$Contrast = \sum_i \sum_j (i-j)^2 P_d(i, j) \tag{4}$$

$$Correlation = \sum_i \sum_j \frac{ijP_d(i, j) - \mu_x \mu_y}{\sigma_x \sigma_y} \tag{5}$$

$$Energy = \sum_i \sum_j P_d^2(i, j) \tag{6}$$

$$Homogeneity = \sum_i \sum_j \frac{P_d(i, j)}{1 + |i-j|} \tag{7}$$

where $P_d(i, j)$ is a pixel in row *i*-th and column *j*-th.

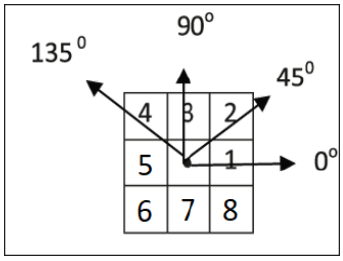

Figure 9. Eight Different Direction Co-Occurrence Matrix

2.4. Segmentation Fractal Texture Analysis (SFTA)

SFTA is a texture feature extraction method that consists of two main steps, the decomposition of the grayscale image (I) into a binary image (I_b) set and three features extraction from each image. Decomposition is a process that converts an input grayscale image into a binary image using a threshold (t) with Equation (8)

$$I_b(x,y) = \begin{cases} 1, t_l < I(x,y) \leq t_u \\ 0, otherwise \end{cases} \quad (8)$$

Where t_l and t_u denote lower and upper threshold values respectively. The multi-level Otsu algorithm is used to find a set of threshold values T, where the length of T is equal to n_t, a user-defined parameter.

After decomposing the image into several binary images, SFTA extracts three features from each binary image, namely binary image's size, mean and boundaries fractal dimension. The regions' boundaries of a binary image $I_b(x,y)$ represented as a border image denoted by $\Delta(x,y)$ and computed with Equation (9):

$$(x,y) = \begin{cases} 1, \exists\,(x',y') \in N_g[(x,y)]:\ I_b[(x',y') = 0 \wedge I_b(x,y) = 1 \\ 0, otherwise \end{cases} \quad (9)$$

Where the set of pixels $N_g(x,y)$ are 8-connected to (x,y), $\Delta(x,y)$ have value 1 if the position (x,y) of the pixel in the corresponding binary image $I_b[(x,y)$ has the value 1 and having at least one neighboring pixel with value 0, otherwise, $\Delta\,(x,y)$ takes the amount 0 [16].

2.5. K-Nearest Neighbors (KNN)

KNN is a method for classifying objects based on learning data that closest to the object, with K is number of some neighbors that are closest to the object. The distance of neighbors is usually calculated based on Euclidean distance. Learning data is projected onto many-dimensional spaces with each dimension represents a feature of the data, the space divided into sections based on the classification. If class "A" is the most common classification of the nearest neighbors of the point, then a point in this space is marked by class "A" [17]. Two-dimensional KNN illustrated in Figure 10.

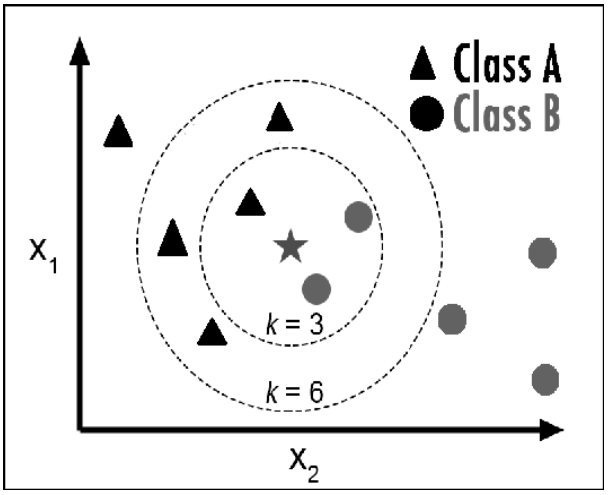

Figure 10. Two Dimensional (X_1, X_2) KNN, with K= 3 and K= 6

2.6. Support Vector Machine (SVM)

Support vector machine (SVM) is a technique for making predictions in cases of classification and regression. The purpose of the SVM Technique is to find the best classifier function (hyperplane) among some unlimited functions to separate two classes. Finding the best hyperplane is equivalent to maximizing the distance between two sets of objects from different classes. Linear hyperplane can be seen in Figure 11.

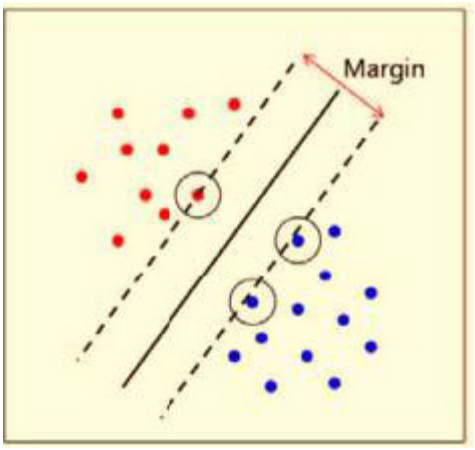

Figure 11. A hyperplane of SVM Classification [18]

For classification problem can be formulated sets of parameters (w, b) so that

$$min_{w,b} = \frac{1}{2} w^T w \tag{10}$$

Subject to

$$y_k = (wx_k + b) \geq 1, \forall x$$

Where vector w and the constant b parameterize the separating hyperplane and x is input vector. In this work, we use linear and RBF SVM kernels for classification [12].

The formula of RBF Kernel with equation (11).

$$K(x_i, y_j) = exp(-\gamma \| x_i - x_j \|^2), \gamma \geq 0 \tag{11}$$

Where γ is hyperparameter. While linear kernel formulated as follow

$$K(x_i, y_j) = \phi(x_i)^T . \phi(x_i) \tag{12}$$

3. Results and Discussion

After each image beeing converted into grayscale then we enhance it by using contrast limited adaptive histogram equalization. Then we do feature extraction using GLCM, LBP, and SFTA.

In this study, the value of feature extraction using GLCM can be seen in Table I. From Table I, two features (correlation and homogeneity) of GLCM show similar value for each image. While in LBP, we set the radius to 1 and the number of neighbors is 8. In this study, LBP produces 256 features from each image. Then, we also compare GLCM and LBP features with SFTA features. In SFTA, our method produces nine features which using $n_t = 2$.

No Sample	Contrast	Correlation	Energy	Homogenity
1	2,56E+04	9,87E+05	2,74E+05	9,87E+05
2	2,22E+04	9,92E+05	2,22E+05	9,89E+05
3	1,99E+04	9,90E+05	2,96E+05	9,90E+05
4	2,31E+04	9,89E+05	2,56E+05	9,88E+05

5	2,76E+04	9,81E+05	3,17E+05	9,86E+05
6	3,48E+04	9,89E+05	2,63E+05	9,83E+05
7	2,66E+04	9,86E+05	2,66E+05	9,87E+05
8	1,86E+04	9,83E+05	3,50E+05	9,91E+05
9	3,49E+04	9,82E+05	2,84E+05	9,83E+05
10	2,64E+04	9,87E+05	3,77E+05	9,87E+05
11	1,56E+04	9,89E+05	5,83E+05	9,92E+05
12	7,49E+03	9,94E+05	6,64E+05	9,96E+05
13	2,33E+04	9,93E+05	2,56E+05	9,88E+05
14	2,74E+04	9,83E+05	3,15E+05	9,86E+05
15	3,29E+04	9,82E+05	3,47E+05	9,84E+05

Table 1 . Performance Of Glcm Measurement (For 15 Images Sample)

The learning and classification process is done using two methods, KNN and SVM. From the previous work [7], the higher accuracy obtained in splitting data 70:30. So, we split the data 70:30 where 70% for training and the rest for testing. In this study, we choose the RBF kernel for SVM and $k = 1$ for KNN. Accuracy calculated as performance measurement from the experiment.

$$Accuracy = \frac{TP + TN}{TP + TN + FP + TN} \tag{13}$$

where

TP = Abnormal classified correctly by the classifier

TN = Normal eye classified correctly by the classifier

FP = Normal eye classified wrongly by classifier

FN = Abnormal classified wrongly by the classifier.

Experimental results in this study can be seen in Table II and Table III. From Table II, the classification using SVM show that GLCM outperformed than other to detect redsmalldots and neovascularization. While LBP has similar accuracy value with GLCM to detect soft exudates and redsmalldots i.e. 68.42% and 81.58% respectively. SFTA only has higher accuracy to detect hard exudates than others.

In Table 3, experimental results show that SFTA has higher accuracy for whole lesion characteristics class, exception haemorrhages class. For haemorrhages class, LBP outperformed than others in KNN classifier.

	SVM		
	GLCM	**LBP**	**SFTA**
Redsmalldots	**81.58%**	**81.58%**	76.31%
Haemorrhages	61.53%	**69.23%**	61.53%
Hard exudates	55.26%	63.16%	**73.68%**
Soft exudates	**68.42%**	**68.42%**	65.79%
Neovascularization	**86.84%**	78.94%	76.31%

Table 2. Performance Svm Measurement Accuracy

In general, KNN classifier is better than SVM, this indicates that similarity between the same lesion is high for each image. Neovascularization detection accuracy is higher than the other, and it indicates that neovascular lesion is natural characteristics to distinguish between neovascular and the other lesion as well as between normal and diabetic retinopathy.

From classification results, we noticed that neovascularization is an important lesion characteristic to detect diabetic retinopathy (especially in Proliferative diabetic retinopathy (PDR) stages). From Table III (KNN classifier), we get that SFTA and LBP give higher accuracy for the whole classification than GLCM approaches.

In Table 4, we make a comparison from our results and previous work. We choose the higher accuracy of each class to describe that the proposed method is good from other works. Other researchers detect exudates lesion to classify abnormal and normal retina, while we manage to detect some lesion characteristics of diabetic retinopathy such as exudates, redsmalldots, haemorrhages, and neovascularization. Our proposed method has higher accuracy in neovascularization (96%) and redsmalldots (92%). We also got 88% accuracy for exudates, and it is lower than other previous work because the different of data was used.

	KNN		
	GLCM	**LBP**	**SFTA**
Redsmalldots	80%	88%	**92%**
Haemorrhages	69.23%	**88.46%**	80.77%
Hard exudates	76%	80%	**88%**
Soft exudates	68%	76%	**76%**
Neovascularization	92%	88%	**96%**

Table 3. Performance Knn Measurement Accuracy

Method	**Data**	**Accuracy**	**Lesion Characteristics**
Ravishankar [5]	STARE database	95,7%	Exudates
Kumari [6]	Personal data	92%	Neovascularization Exudates
Ram [8]	DiaretDB1	88%	Haemorrhages
Our proposed	DiaretDB0	88% 96% 92% 88,46%	Exudates Neovascularization Red small dots Haemorhages

Table 4. Comparison of Results for Lesion Characteristics

4. Conclusions

This paper has presented a comparison of several combinations of feature extraction methods and classification methods to analyze lesion characteristics in diabetic retinopathy. From our results, we can conclude that among many combinations of feature extraction and classifier, the combination of SFTA (feature extraction) and KNN (classifier) is the best approach for detecting lesion characteristics of diabetic retinopathy. Other results show that neovascular lesion characteristics are the best lesion descriptor to distinguish normal and diabetic retinopathy. For future works, we could combine texture features and lesions characteristics as information to analyze big data images and other medical images. We can also improve the performance using

advanced computing.

Acknowledgment

This work supported by PDUPT 2018 grant from Directorate General of Higher Education Indonesia, in the help of DRPM Universitas Indonesia.

References

[1] Definition, diagnosis, and classification of diabetes mellitus and its complications. Part 1: Diagnosis and classification of diabetes mellitus. World Health Organization, Geneva, 1999. Report Number: WHO/NCD/NCS/99.2

[2] Yau, J.W., Rogers, S.L., et al. (2012). Global prevalence and major risk factors of diabetic retinopathy, *Diabetes Care*; 35(3) 556-64.

[3] Usman Akram, M., Khalid, S., Tariq, A., Khan, S.A., Azam. F. (2014). Detection and classification of retinal lesions for grading of diabetic retinopathy, *Computers in Biology and Medicine*, 45 (1) 161–171, 2014.

[4] Narasimhan, K., Neha, V. C., Vijayarekha. K. (2012). An Efficient Automated System for Detection of Diabetic Retinopathy from Fundus Images Using Support Vector Machine and Bayesian Classifiers, *In*: IEEE Transl. International Conference on Computing, Electronics and Electrical Technologies (ICCEET), Kumaracoil, 2012. p. 964-969.

[5] Ravishankar, S. A., Jain., Mittal, A. (2009). Automated Feature Extraction for Early Detection of Diabetic Retinopathy in Fundus Images, *In*: IEEE Transl. International Conference on Computer Vision and Pattern Recognition (CVPR), 2009, p 210-217.

[6] Kumari, V.V., Suriyanarayanan, N., Thanka Saranya, C. (2010). Feature Extraction for Early Detection of Diabetic Retinopathy, *In*:IEEE Transl. International Conference on Recent Trends in Information, Telecommunication and Computing, 2010, p. 359-361.

[7] Abdillah, B., Bustamam, A., Devvi, S. (2017). Classification of Diabetic Retinopathy Through Texture Features Analysis, *In*: 2017 International Conference on Advanced Computer Science and Information Systems, Bali, Indonesia, 2017, p. 333-337.

[8] Ram, K., Joshi, G. D., Sivaswamy, J. (2011). A successive clutter-rejection-based approach for early detection of diabetic retinopathy, *In*: IEEE Transactions on Biomedical Engineering, 2011, 58 (3 PART 1) 664–673.

[9] Kauppi, T., Kalesnykiene, V., Kamarainen, J., Lensu, L., Sorri, I., Uusitalo, H., Kalviainen, H., Pietila, J. DIARETDB0: Evaluation Database and Methodology for Diabetic Retinopathy Algorithms, Technical report.

[10] Datta, N. S., Dutta, H. S., De, M., Mondal, S. (2013). An Effective Approach: Image Quality Enhancement for Microaneurysms Detection of Non-dilated Retinal Fundus Image. *Procedia Technology*. 10, 731–737.

[11] Ojala, T., Pietikainen, M., Harwood, D. (1996). A Comparative Study of Texture Measures with Classification Based on Feature Distributions, *Pattern Recognition*, 29 (1) 51-59.

[12] Sarwinda, D., Bustamam, A. (2016). Detection of Alzheimer's disease using advanced local binary pattern from hippocampus and whole brain of MR images, *In*: 2016 International Joint Conference on Neural Networks (IJCNN), 5051–5056.

[13] Meena, K., Suruliandi, A. (2011). Local Binary Patterns and its Variants for face Recognition, *In:* IEEE-International Conference on Recent Trends in Information Technology (ICRTIT), 2011, Chennai, 782-786.

[14] Ahonen, T., Hadid, A., Pietikainen, M. (2006). Face Description with Local Binary Patterns: *Application to Face Recognition, IEEE Transactions on Pattern Analysis and Machine Intelligence*, 28 (12) 2037-2041, Dec. 2006.

[15] Xie, Z. X. Z., Liu, G. L. G., He, C. H. C., and Wen, Y. W. Y. (2010). Texture Image Retrieval Based on Gray Level Co-Occurrence Matrix and Singular Value Decomposition, *In*: 2010 International Conference on Multimedia Technology (ICMT), 2010, (1) 3–5.

[16] Costa, A.F., Humpire-Mamani, G., and Traina, A.J.M. (2012). An efficient algorithm for fractal analysis of textures, *In*: Brazilian Symposium of Computer Graphic and Image Processing, 2012, 39–46.

[17] Mirajkar, S., and Patil, M.M. (2013). Feature Extraction of Diabetic Retinopathy Images, *International Journal of Computer Applications (IJCA), In:* Proceedings on Emerging Trends in Electronics and Telecommunication Engineering (Ncet), 2013, 5–8.

18] Nasser, A.T., Dogru, N. (2017). Signature recognition by using SIFT and SURF with SVM basic on RBF for voting online, *In:* 2017, International Conference on Engineering and Technology (ICET), 2017. Antalya, Turkey.